

1.72 and 2.33 Å; the lower limit is typical of those occurring in MoO<sub>4</sub> tetrahedra but it has been reported for MoO<sub>6</sub> octahedra in the structure of sodium dimolybdate (Lindquist, 1950a).

Inter-cation distances (Table 4, Fig. 3a) also show wide variation, particularly for the edge-sharing octahedra. Distances between cations in octahedra which share corners either within a chain, *e.g.* Co(1)–Mo(1), Mo(2)–Co(2) or between chains, *e.g.* Mo(1)–Co(2) and Co(1)–Mo(2), are close to those found in the complex molybdenum oxides, Mo<sub>8</sub>O<sub>23</sub> and Mo<sub>9</sub>O<sub>26</sub> (Magnéli, 1948), though less than those reported in the complex ions (Mo<sub>7</sub>O<sub>24</sub>)<sup>6-</sup> and (Mo<sub>8</sub>O<sub>26</sub>)<sup>4-</sup> (Lindquist, 1950b). On the other hand, the cation distances for the edge-sharing octahedra show a very wide range of distances. Extreme values arise between like cations: *e.g.* Mo(2)–Mo(2) = 3.80 Å compared with Co(1)–Co(2) = 3.07 Å. Other intercation distances compare favorably with those in the complex para- and tetra-molybdate ions.

Why these displacements of the cations from the centers of their octahedra occur is not known, but a study of the magnetic and electrical properties of CoMoO<sub>4</sub> might possibly provide pertinent information. There are very few well-refined complex oxide structures reported in the literature, and we believe that the displacements found here are probably more common than one would suspect on the basis of the classic oxide structures, many of which are sorely in need of redetermination or refinement.

It has been reported (Smith, 1962) that nickel molybdate is isomorphous with cobalt molybdate and simple attempts have been made to synthesize the other molybdates of small cations such as Fe, Mg, Mn, and Zn. The X-ray powder photographs of these molybdates all gave exceedingly complex patterns all differing from each other. As the valency state of the iron and manganese in the starting materials was uncertain,

the composition of the iron and manganese compounds is in doubt.

However, Young (1964) reports that at ambient pressures MnMoO<sub>4</sub> and MgMoO<sub>4</sub> give similar diffraction patterns but that ZnMoO<sub>4</sub> and FeMoO<sub>4</sub> each give unique patterns. It is also reported (Young & Schwartz, 1963) that when the small-cation molybdates are synthesized at high pressures and temperatures the stable structure is of the wolframite type with cell parameters, in each case, very close to those of the tungstate analogues; but after prolonged heating at 600°C reversion takes place to their respective structures at ordinary pressures.

The early calculations were made on a DEUCE computer, using programs written by Dr Rollett, and on an Elliott 803. Thanks are due to Mr D. J. Smith, who made the calculations, for his structure-factor program for the Elliott machine.

We wish to thank the Chairman and Directors of the British Petroleum Company Limited for permission to publish this paper.

#### References

- HAMILTON, W. C. (1965). *Acta Cryst.* **18**, 502.  
 IBERS, J. A. (1962). In *International Tables for X-ray Crystallography*, Vol. III, Table 3.3. 1A. Birmingham: Kynoch Press.  
 IBERS, J. A. & HAMILTON, W. C. (1964). *Acta Cryst.* **17**, 781.  
 KEELING, R. O. (1957). *Acta Cryst.* **10**, 209.  
 LINDQUIST, I. (1950a). *Acta Chem. Scand.* **4**, 1066.  
 LINDQUIST, I. (1950b). *Ark. Kemi*, **2**, 325, 349.  
 MACKAY, A. L. (1953). *Acta Cryst.* **6**, 214.  
 MAGNÉLI, A. (1948). *Acta Chem. Scand.* **2**, 501.  
 SMITH, G. W. (1962). *Acta Cryst.* **15**, 1054.  
 TEMPLETON, D. H. (1962). In *International Tables for X-ray Crystallography*, Vol. III, Table 3.3.2C. Birmingham: Kynoch Press.  
 YOUNG, A. P. (1964). Private communication.  
 YOUNG, A. P. & SCHWARZ, C. M. (1963). *Science*, **141**, 348.

### Short Communications

*Contributions intended for publication under this heading should be expressly so marked; they should not exceed about 1000 words; they should be forwarded in the usual way to the appropriate Co-editor; they will be published as speedily as possible. Publication will be quicker if the contributions are without illustrations.*

*Acta Cryst.* (1965). **19**, 275

**Stannides and plumbides of Sc, Y, La and Ce with D<sub>8h</sub> structure.** By W. JEITSCHKO and E. PARTHÉ, *Metallurgy Department, Laboratory for Research on the Structure of Matter, University of Pennsylvania, Philadelphia, Pa., U.S.A.*

(Received 10 December 1964)

#### Introduction

In the past not much attention has been paid to the alloy formation between scandium, yttrium or rare earth elements and tin or lead as second components. AB<sub>3</sub> compounds with

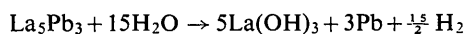
Cu<sub>3</sub>Au structure type were the only compounds reported which have been analyzed structurally. Partial phase diagrams have been reported for La–Pb (Cannery, 1931) and Ce–Pb (Vogel & Heumann, 1943) based mostly on metallo-

graphic and thermal analysis studies. These two diagrams show compounds with the composition  $(RE)_2Pb$  ( $RE =$  rare earth element) as the only compound between 50 and 100 at. %  $RE$ . However, X-ray studies in related systems demonstrated that phases with composition  $(RE)_2X_3$  occur with silicides and germanides of scandium, yttrium and rare earth elements (Parthé, 1960; Arbuckle & Parthé, 1962; Baenziger & Hegenbarth, 1964) and the formation of homolog stannides and plumbides appeared likely. In view of this disagreement between structural studies on silicides and germanides and the result of the phase diagram studies of lead systems, an X-ray investigation of alloys with composition  $(Sc, Y, La, Ce)_5(Sn, Pb)_3$  seemed to be of interest.

### Sample preparation

The starting materials used were 99.9% cerium, 99.9% lanthanum, 99% scandium, 99.99% lead and 99.9% tin. The alloy specimens were prepared by arc melting stoichiometric mixtures of the metals. On first sight this method might not seem appropriate since the melting points, for example, of scandium (1539°C) and lead (327°C) are more than 1000° apart; however, the boiling point of the lower melting metal (lead 1725°C, tin 2270°C) was always above the melting point of scandium, yttrium or cerium and lanthanum. Purgon (purified argon) was used as inert atmosphere during the melting process, and a titanium button was melted prior to each melt. After remelting every sample twice, some specimens were annealed for homogenizing in evacuated quartz tubes for 400 hours at 600°C. However, it was found that the last step was not really necessary as the samples were found to be homogeneous, even with the arc melting alone.

All samples investigated were rapidly attacked by the water vapor of the air. Therefore, it was necessary to keep the samples in a desiccator. The specimens were ground under ligroin which had been dried with metallic sodium. For the X-ray diffraction experiments, the ground material was put into capillaries and X-rayed while still under dried ligroin. When exposed to moist air, the alloy powder reacts rapidly with the formation of hydrogen. The hydrolysis reaction in the case of  $La_5Pb_3$  is probably as follows:



Only diffraction lines of hexagonal  $La(OH)_3$  (Roy & McKinstry, 1953) and elementary Pb were observed in the reaction product of  $La_5Pb_3$ . In the case of  $Y_5Sn_3$  and  $Y_5Pb_3$ , only Sn and Pb lines were observed and the hydroxide of Y was present in an amorphous form. Interestingly enough, no oxide lines of lead or tin could be observed in any of these films.

### Structure of $Sc_5Pb_3$

A powder diffraction pattern of  $Sc_5Pb_3$  could be indexed with a hexagonal unit cell of:

$$a = 8.467 \pm 0.004, \quad c = 6.158 \pm 0.003 \text{ \AA}.$$

The extinctions for  $h0hl$  with  $l = 2n + 1$  lead to possible space groups  $P6_3/mcm$  ( $D_{6h}^3$ ),  $P6c2$  ( $D_{3h}^2$ ),  $P6_3cm$  ( $C_{6v}^3$ ),  $P3c1$  ( $D_{3d}^4$ ) and  $P3c1$  ( $C_{3v}^3$ ). The pattern of  $Sc_5Pb_3$  resembles the pattern for  $(Ti, Zr)_5Pb_3$  which has been reported to crystallize with the  $D8_8$  structure (Nowotny, Auer-Welsbach, Bruss & Kohl, 1959). Therefore, in the first trial space group  $P6_3/mcm$  ( $D_{6h}^3$ ) was chosen and 4Sc atoms were placed in position 4(d), 6Sc in 6(g)<sub>I</sub> with  $x_I = 0.25$  and 6Pb in 6(g)<sub>II</sub> with  $x_{II} = 0.61$ . The calculated intensities agreed rather

well with the observed intensities which showed that the structure of  $Sc_5Pb_3$  is of the  $D8_8$  structure type. However, efforts were made to change the adjustable parameters in order to improve the agreement. The intensities of a powder film were measured and corrected for absorption (Bradley, 1935). An absorption correction was necessary here, since – as described above – capillaries had to be used for the powder photograph. The best fit between observed and calculated values was obtained for an  $x_I$  value of  $0.24 \pm 0.01$  for the Sc atoms in position 6(g)<sub>I</sub> and an  $x_{II}$  value of  $0.606 \pm 0.002$  for the Pb atoms in positions 6(g)<sub>II</sub>. Owing to the larger scattering power of lead, the parameter value of the latter could be determined more accurately than that for scandium. Table 1 shows the intensity calculation for  $Sc_5Pb_3$  with these parameters.

### Isotypic stannides and plumbides

The powder patterns of  $Sc_5Sn_3$ ,  $Y_5Sn_3$ ,  $Y_5Pb_3$ ,  $La_5Pb_3$ , and  $Ce_5Pb_3$  could be indexed with similar hexagonal unit cells. The lattice constants, axial ratios and calculated densities are given in Table 2. The intensities of the diffraction lines of  $Y_5Sn_3$ ,  $La_5Pb_3$  and  $Ce_5Pb_3$  agreed very well with those

Table 1. Intensity calculation for  $Sc_5Pb_3$  with  $D8_8$  structure (Cr  $K\alpha$  radiation)

hkl	$d_c$ (Å)	$10^3 \cdot \sin^2 \theta_o$	$10^3 \cdot \sin^2 \theta_o$	$l_c$	$l_o$
10 $\bar{1}$ 0	7.333	24.4	*	2.66	*
1 $\bar{1}$ 20	4.233	73.2	73.8	2.95	2.5
2020	3.667	97.6	97.9	1.81	2
1 $\bar{1}$ 21	3.488	107.8	107.8	10.00	10
0002	3.079	138.4	138.1	3.94	4
10 $\bar{1}$ 2	2.839	162.8	-	0.16	-
2130	2.771	170.8	171.2	0.63	0.5
2 $\bar{1}$ 31	2.528	205.4	205.6	7.77	8
1122	2.490	211.6	211.4	4.82	4
3030	2.444	219.6	219.3	3.41	3.5
2022	2.358	236.0	236.6	2.32	2.5
2240	2.117	292.8	-	0.02	-
2132	2.060	309.2	-	0.04	-
3140	2.034	317.2	317.5	1.14	1
2241	2.002	327.4	327.4	1.65	1.5
3141	1.931	351.8	351.5	4.39	4.5
3032	1.914	358.0	358.4	1.36	1
1123	1.847	384.6	384.4	1.76	2
4040	1.833	390.4	-	0.04	-
2242	1.780	431.2	431.9	0.48	0.5
3142	1.697	455.6	455.8	0.66	0.6
3250	1.682	463.6	463.4	0.65	0.6
2133	1.650	482.2	482.8	2.29	2.5
3251	1.623	498.2	497.8	0.19	0.2
4150	1.600	512.4	-	0.00	-
4042	1.575	528.8	-	0.00	-
4151	1.549	547.0	547.2	0.11	0.2
0004	1.539	553.6	553.6	0.95	0.8
1014	1.507	578.0	578.3	0.11	0.2
3252	1.476	602.0	603.1	1.91	2.5
2243	1.474	604.2	604.2	0.87	1
5050	1.467	610.0	610.4	1.65	1.5
1124	1.447	626.8	628.1	0.43	3.5
3143	1.445	628.6	628.6	2.59	3
4152	1.420	650.8	651.4	0.47	1
2024	1.419	651.2	-	0.41	-
3360	1.411	658.8	-	0.02	-
4260	1.386	683.2	683.4	1.01	1
3361	1.376	693.4	693.4	0.83	0.9
4261	1.352	717.8	717.2	3.20	3
2134	1.346	724.4	725.0	0.22	0.2
5052	1.324	748.4	748.1	4.61	4.5
5160	1.317	756.4	756.3	0.23	0.2
3034	1.303	773.2	-	2.18	-
3253	1.301	775.0	773.6	0.18	2.5
5161	1.288	791.0	790.8	0.33	0.4
3362	1.283	797.2	-	0.09	-
4262	1.264	821.6	822.1	1.52	1.5
4153	1.262	823.8	-	0.13	-
2244	1.245	846.4	-	0.03	-
3144	1.227	870.8	870.8	1.77	2
6060	1.222	878.4	-	0.00	-
5162	1.211	894.8	-	0.17	-
4370	1.206	902.8	-	0.18	-
4371	1.183	937.4	937.9	3.56	8
1125	1.183	938.2	-	2.70	-
4044	1.179	944.0	-	0.14	-
5270	1.174	951.6	951.6	1.84	2
3363	1.163	970.2	970.1	2.58	4

\* ) not observed

Table 2. Lattice constants and theoretical densities of  $D8_8$  phases

Compound	$a$	$c$	$c/a$	$\rho$
$\text{Sc}_5\text{Sn}_3$	$8.408 \pm 0.004 \text{ \AA}$	$6.081 \pm 0.003 \text{ \AA}$	$0.7232 \pm 0.0005$	$4.65 \text{ g.cm}^{-3}$
$\text{Sc}_5\text{Pb}_3$	$8.467 \pm 0.004$	$6.158 \pm 0.003$	$0.7273 \pm 0.0005$	6.45
$\text{Y}_5\text{Sn}_3$	$8.878 \pm 0.005$	$6.516 \pm 0.004$	$0.7339 \pm 0.0005$	5.53
$\text{Y}_5\text{Pb}_3$	$8.971 \pm 0.004$	$6.614 \pm 0.003$	$0.7373 \pm 0.0003$	6.93
$\text{La}_5\text{Pb}_3$	$9.528 \pm 0.005$	$6.993 \pm 0.003$	$0.7339 \pm 0.0006$	7.32
$\text{Ce}_5\text{Pb}_3$	$9.473 \pm 0.004$	$6.825 \pm 0.002$	$0.7204 \pm 0.0004$	7.63

for  $\text{Sc}_5\text{Ga}_3$  (Schob & Parthé, 1964) and the intensities of  $\text{Sc}_5\text{Sn}_3$  and  $\text{Y}_5\text{Pb}_3$  were similar to those of  $\text{Zr}_5\text{Pb}_3$  (Nowotny & Schachner, 1953). All five compounds, therefore, crystallize with the  $D8_8$  structure type. The  $d$  values and the intensities observed with chromium  $K\alpha$  radiation for the five compounds are listed in Table 3\*.

### Conclusion

The X-ray study has demonstrated that the published phase diagrams for La–Pb and Ce–Pb are not complete, since the phases  $\text{La}_5\text{Pb}_3$  and  $\text{Ce}_5\text{Pb}_3$  do not appear in the diagrams. An additional correction is necessary for the diagram Ce–Pb, since it was shown recently that a compound  $\text{Ce}_3\text{Pb}$  exists which crystallizes with a  $\text{Cu}_3\text{Au}$  structure (Jeitschko, Nowotny & Benesovsky, 1964). Therefore, in the system Ce–Pb there occur two compounds with the  $\text{Cu}_3\text{Au}$  structure, one having composition  $\text{Ce}_3\text{Pb}$ , the second  $\text{CePb}_3$ . (Zintl & Neumayr, 1933).

The six new compounds reported here increase the number of known  $D8_8$  phases to more than fifty. The available results indicate that the  $D8_8$  structure occurs with transition metals of the third to the eighth group as one partner and B elements of the third, fourth and fifth group as the second component. The structure can accommodate a very wide range of size differences of the participating atoms. The size ratio varies from 0.83 for  $\text{Ti}_5\text{Pb}_3$  to 1.35 for  $\text{Y}_5\text{Si}_3$ . A more detailed study on the characteristics of the  $D8_8$  structure type and its variations will appear in the near future.

This study is a contribution from the Laboratory for Research on the Structure of Matter, University of Pennsylvania, supported by the Advanced Research Projects Agency, Office of the Secretary of Defence.

### References

- ARBUCKLE, J. & PARTHÉ, E. (1962). *Acta Cryst.* **15**, 1205.  
 BAENZIGER, N. C. & HEGENBARTH, J. J. (1964). *Acta Cryst.* **17**, 620.  
 BRADLEY, A. J. (1935). *Proc. Phys. Soc.* **47**, 879.  
 CANNERI, G. (1931). *Metallurgia ital.* **23**, 805.  
 HOLMEN, S. (1964). *Acta Chem. Scand.* **18**, 2394.  
 JEITSCHKO, W., NOWOTNY, H. & BENESOVSKY, F. (1964). *Mh. Chem.* **95**, 1040.  
 NOWOTNY, H., AUER-WELSBACH, H., BRUSS, J. & KOHL, A. (1959). *Mh. Chem.* **90**, 15.  
 NOWOTNY, H. & SCHACHNER, H. (1953). *Mh. Chem.* **84**, 169.  
 PARTHÉ, E. (1960). *Acta Cryst.* **13**, 868.  
 ROY, R. & MCKINSTRY, H. A. (1953). *Acta Cryst.* **6**, 365.

\* Note added in proof. – The compound  $\text{Y}_5\text{Sn}_3$  has been found recently also by Holmen (1964), who reports the same structure type but slightly larger unit-cell constants.

- SCHOB, O. & PARTHÉ, E. (1964). *Acta Cryst.* **17**, 1335.  
 VOGEL, R. & HEUMANN, F. (1943). *Z. Metallk.* **35**, 29.  
 ZINTL, E. & NEUMAYR, S. (1933). *Z. Elektrochem.* **39**, 86.

Table 3.  $d$  values and observed intensities (Cr  $K\alpha$  radiation) for new compounds with  $D8_8$  structures

$\text{Sc}_5\text{Sn}_3$	$\text{Y}_5\text{Sn}_3$	$\text{Y}_5\text{Pb}_3$	$\text{La}_5\text{Pb}_3$	$\text{Ce}_5\text{Pb}_3$
$hkl$ $d_c$ (Å) $I_o$	$hkl$ $d_c$ (Å) $I_o$	$hkl$ $d_c$ (Å) $I_o$	$hkl$ $d_c$ (Å) $I_o$	$hkl$ $d_c$ (Å) $I_o$
100 7.281 v	100 7.689 v	100 7.769 v	100 8.251 v	100 8.204 v
110 4.204 -	110 4.441 vw	110 4.485 vw	110 4.766 -	110 4.756 -
200 3.640 vvw	200 3.845 -	200 3.885 -	200 4.126 -	200 4.131 -
111 3.459 w	111 3.649 vw	111 3.713 w	111 3.938 vvw	111 3.891 vw
002 3.040 -	002 3.258 -	002 3.307 -	002 3.497 vw	002 3.413 w
102 2.806 -	102 3.000 vvw	102 3.043 -	102 3.219 -	102 3.180 -
210 2.752 vvw	210 2.906 vw	210 2.937 vw	210 3.120 vvw	210 3.100 vw
211 2.507 ms	211 2.654 s	211 2.684 s	211 2.848 s	211 2.824 s
112 2.464 m	112 2.626 s	112 2.662 ms	112 2.819 ms	112 2.769 s
202 2.427 mw	202 2.563 w	202 2.590 m	202 2.751 ms	202 2.735 ms
220 2.333 w	220 2.485 vw	220 2.518 w	220 2.667 mw	220 2.624 w
220 2.102 -	220 2.219 -	220 2.256 -	220 2.382 -	220 2.368 -
212 2.040 -	212 2.169 -	212 2.196 -	212 2.328 -	212 2.295 -
310 2.020 w	310 2.132 vvw	310 2.155 vw	310 2.289 vw	310 2.275 vw
221 1.986 w	221 2.101 vw	221 2.124 w	221 2.255 w	221 2.237 vw
311 1.916 s	311 2.027 w	311 2.049 ms	311 2.175 ms	311 2.158 m
300 1.859 vw	300 2.015 -	300 2.039 ms	300 2.162 ms	300 2.134 -
113 1.826 w	113 1.951 -	113 1.979 vw	113 2.095 vw	113 2.051 vw
400 1.820 w	400 1.922 -	400 1.942 -	400 2.061 -	400 2.050 vw
222 1.729 w	222 1.834 w	222 1.856 mw	222 1.968 w	222 1.966 w
312 1.682 -	312 1.784 -	312 1.804 -	312 1.915 -	312 1.893 -
320 1.671 -	320 1.764 -	320 1.782 vvw	320 1.893 -	320 1.882 -
213 1.632 s	213 1.740 s	213 1.763 ms	213 1.869 ms	213 1.834 s
321 1.611 vw	321 1.705 w	321 1.721 vw	321 1.827 vvw	321 1.812 vvw
410 1.589 -	410 1.678 w	410 1.696 w	410 1.801 -	410 1.790 vw
402 1.562 -	402 1.655 w	402 1.675 vw	402 1.777 vvw	402 1.758 vw
411 1.537 -	411 1.629 m	411 1.649 mw	411 1.748 m	411 1.732 -
004 1.520 w	411 1.625 -	411 1.642 -	411 1.744 m	004 1.706 w
104 1.488 -	104 1.594 -	104 1.617 -	104 1.710 -	104 1.702 w
322 1.464 m	223 1.552 mw	223 1.572 m	223 1.668 m	322 1.648 m
223 1.459 m	322 1.551 mw	322 1.569 m	322 1.665 m	500 1.661 m.d.
500 1.456 m	500 1.538 w	500 1.561 m	500 1.650 w	223 1.641 vw
313 1.431 m	114 1.529 -	114 1.552 mw	114 1.641 -	313 1.609 w
114 1.410 m	313 1.522 vw	313 1.541 m	313 1.635 m	114 1.605 -
412 1.408 vw	204 1.500 -	204 1.521 -	204 1.609 -	412 1.588 vvw
204 1.403 -	412 1.492 vvw	412 1.509 vw	412 1.601 vw	330 1.579 vvw
330 1.401 -	330 1.480 -	330 1.495 -	330 1.588 -	204 1.575 vvw
420 1.376 w	420 1.453 w	420 1.468 w	420 1.559 vw	420 1.550 vw
331 1.365 w	331 1.443 w	331 1.458 w	331 1.548 vw	331 1.540 vw
421 1.342 s	214 1.421 m.d.	214 1.441 vvw	214 1.523 ms	421 1.512 w
214 1.331 vw	421 1.410 m.d.	421 1.433 m	421 1.521 ms	214 1.495 vw
502 1.313 vs	502 1.391 s	502 1.406 s	502 1.492 s	502 1.479 m.d.
510 1.308 -	510 1.381 -	510 1.395 ms	510 1.482 ms	510 1.474 m.d.
323 1.289 v	304 1.375 m.d.	304 1.394 m	304 1.473 m.d.	323 1.450 s
304 1.285 vw	323 1.368 m.d.	323 1.386 vvw	323 1.472 m	304 1.447 s
511 1.278 vvw	511 1.351 m	511 1.365 w	511 1.450 vw	511 1.440 vvw
332 1.273 -	332 1.347 m.d.	332 1.362 w	332 1.446 vw	332 1.433 m
422 1.254 m	413 1.328 w	413 1.344 w	413 1.427 -	422 1.412 vw
413 1.251 -	422 1.327 vw	422 1.342 w	422 1.424 w	413 1.407 vw
224 1.232 -	224 1.313 s	224 1.331 -	224 1.409 -	224 1.384 -
314 1.215 m	314 1.295 w	314 1.312 w	314 1.389 w	314 1.367 -
600 1.214 -	600 1.281 -	600 1.295 -	600 1.375 -	314 1.365 vw
512 1.201 -	512 1.271 -	512 1.286 -	512 1.365 -	512 1.351 -
430 1.197 -	430 1.264 -	430 1.277 -	430 1.357 -	430 1.349 -
431 1.174 s	115 1.250 -	115 1.269 vw	115 1.342 vvw	431 1.321 vvw
115 1.168 w	404 1.243 -	404 1.259 -	404 1.334 -	520 1.314 -
404 1.167 w	431 1.241 m	431 1.254 m	431 1.332 w	404 1.312 vw
520 1.166 w	520 1.231 vw	520 1.244 w	520 1.321 vvw	115 1.312 m
	333 1.223 m	333 1.237 mw	333 1.315 w	333 1.297 w
	521 1.210 m	521 1.222 ms	521 1.298 ms	521 1.279 vw
	423 1.208 m.d.	423 1.222 s	423 1.298 ms	423 1.281 m
	324 1.197 -	324 1.212 vw	324 1.284 -	602 1.269 vvw
	602 1.193 s.d.	215 1.206 vs	602 1.280 vw	324 1.264 -
	215 1.189 s.d.	602 1.206 vs	215 1.276 ms	432 1.254 -
	432 1.178 -	432 1.191 -	432 1.265 -	610 1.251 vs
		335 1.189 m	335 1.259 w	215 1.249 w
		414 1.184 s	414 1.254 w.d.	513 1.239 w
		513 1.179 vw	513 1.251 w	414 1.235 w.d.
		611 1.166 s	611 1.231 m	611 1.231 m
			522 1.230 w	522 1.224 w.d.
			225 1.206 vw	440 1.184 w
			504 1.200 s	504 1.183 vs
			315 1.191 m	225 1.183 s
			440 1.191 -	612 1.178 w
			612 1.184 w	700 1.172 s
			700 1.170 vw	530 1.172 s
			530 1.170 vw	315 1.170

v) not observed  
 Intensities were not corrected for absorption